Journal of Geophysical Research: Biogeosciences

RESEARCH ARTICLE
10.1029/2017JG004327

Special Section:
Biogeochemistry of Natural Organic Matter

Drivers of Dissolved Organic Matter in the Vent and Major Conduits of the World's Largest Freshwater Spring

Casey Luzius[1], Francois Guillemette[1,2], David C. Podgorski[1,3], Anne M. Kellerman[1], and Robert G. M. Spencer[1]

[1]Department of Earth, Ocean, and Atmospheric Science, Florida State University, Tallahassee, FL, USA, [2]Now at Center for Research on Watershed Interactions-Aquatic Ecosystems, University of Quebec at Trois-Rivieres, Trois-Rivieres, Quebec, Canada, [3]Now at Pontchartrain Institute for Environmental Sciences, Department of Chemistry, University of New Orleans, New Orleans, LA, USA

Abstract Wakulla Springs is the largest and deepest freshwater spring on Earth and has exhibited increased chromophoric dissolved organic matter (CDOM) inputs (i.e., browning) in recent decades. To examine the drivers of changing dissolved organic matter at the spring vent, we examined dissolved organic carbon concentrations and dissolved organic matter composition via optical parameters (i.e., absorbance and fluorescence) in the major conduits and a connecting spring over the course of 1 year. Sample sites separated clearly based on dissolved organic carbon concentration, CDOM absorbance, and optical parameters indicative of autochthonous (clear groundwater) versus allochthonous (terrestrial) dissolved organic matter. Seasonality was apparent in the allochthonous-dominated sites with increasing terrestrial contribution particularly with large precipitation events post dry periods. Principle component analysis highlights the ability of optical parameters to show the dominance of sample sites draining from the southwest (i.e., Apalachicola National Forest) as responsible for the CDOM-rich water at the vent, whereas water draining from the north was comparatively clear. Increasing CDOM-rich waters at the vent suggests that either input from conduits draining from the southwest has increased, or the relative dilution with clear groundwater has decreased in the conduit system prior to discharge from the vent. Sea level rise impacts in the region have been suggested to result in more blackwaters delivered to the vent, and ongoing extraction of clear groundwater reduces the dilution capacity on CDOM-rich waters. Thus, anthropogenic impacts in the region need to be addressed if the trend of increased CDOM inputs at Wakulla Springs is to be reversed.

Key Points:
- Conduits feeding into the spring vent can be separated via optical parameters and linked back to source regions
- Optical measurements that can be made in situ can be utilized to trace the source of chromophoric dissolved organic matter to the vent
- Chromophoric dissolved organic matter at the vent is derived from conduits draining from the southwest (forested areas)

Supporting Information:
- Supporting Information S1

Correspondence to:
R. G. M. Spencer,
rgspencer@fsu.edu

Citation:
Luzius, C., Guillemette, F., Podgorski, D. C., Kellerman, A. M., & Spencer, R. G. M. (2018). Drivers of dissolved organic matter in the vent and major conduits of the world's largest freshwater spring. *Journal of Geophysical Research: Biogeosciences*, *123*, 2775–2790. https://doi.org/10.1029/2017JG004327

Received 27 NOV 2017
Accepted 30 JUL 2018
Accepted article online 7 AUG 2018
Published online 13 SEP 2018

Author Contributions:
Conceptualization: Francois Guillemette, David C. Podgorski
Formal analysis: Casey Luzius, Francois Guillemette, Anne M. Kellerman
Investigation: Casey Luzius, Francois Guillemette, David C. Podgorski
Writing - original draft: Casey Luzius

1. Introduction

Karst landscapes cover approximately 10% of the Earth's land surface, and their aquifers provide a complete or partial source of drinking water to almost a quarter of the global population (Hartmann et al., 2014). Karst aquifers are formed through the dissolution of limestone, dolomite, and other soluble rocks, which creates high permeability and porosity areas (Bush & Johnston, 1988). Globally, karst landscapes are typified by extensive drainage systems connecting surface and subsurface hydrology, including sinkholes and conduit networks that create a highly dynamic hydrologic system. Due to the high level of hydrological connectivity in karst aquifers, land cover plays a major role in determining water quality. For example, previous studies have highlighted contaminants linked to increasing urbanization, such as chemicals associated with pharmaceuticals and personal care products, as well as agricultural fertilizers impacting karst aquifers (Barnes et al., 2008; Focazio et al., 2008; Hartmann et al., 2014; Katz & Griffin, 2008). Due to the hydrological complexity of karst aquifers, they are generally understudied, and there is currently limited understanding with respect to their role in biogeochemical cycling despite their importance as sites of groundwater-surface water interactions (Hartmann et al., 2014; Sophocleous, 2002).

Karst springs are formed where groundwater flow discharges from a conduit or cave at a vent and becomes surface water. Springs have been observed to typically have high water clarity and stable hydrology, chemistry, and temperature (Berndt et al., 1998), yet in recent decades, numerous springs in the southern United States of America (USA), including Wakulla Springs, have experienced a change in water color (browning) and shifts in ecology (Arellano & Coble, 2015; Florida Geological Survey Publication 58, 2005; Musgrove et al., 2016). Wakulla Springs is the largest and deepest freshwater spring on Earth and represents a prime example of a site-facing problems common to many spring systems in the southern United States. Specifically, in

recent decades Wakulla Springs has seen increased nutrient loading (e.g., a fivefold increase in nitrate loading in less than 30 years from the 1970s through the 1990s) as well as an increase in inputs from sources of chromophoric dissolved organic matter (CDOM, Florida Geological Survey Publication 58, 2005). These negative impacts to the water quality at Wakulla Springs have ramifications not just for the biogeochemistry and ecology of the system but also for the approximate 200,000 recreational visitors to the Wakulla Springs each year.

Dissolved organic matter (DOM) is a complex mixture of soluble organic compounds that play a wide variety of roles in aquatic ecosystems and take part in biological, chemical, and physical transformations (Aiken et al., 2011; Fellman et al., 2010; Jaffé et al., 2008). The fraction of DOM that absorbs ultraviolet and visible light is known as CDOM, and a smaller portion of CDOM that fluoresces is termed fluorescent dissolved organic matter (FDOM) (Baker & Spencer, 2004; Coble et al., 1990; Fellman et al., 2010). Surface waters typically contain DOM from different sources, such as terrestrial soils and vegetation (allochthonous), anthropogenic (e.g., agricultural, sewage, and wastewater), and autochthonous origins (e.g., algae, macrophytes, and microbial) (Baker & Spencer, 2004; Birdwell & Engel, 2010; McKnight et al., 2001). As shown in a broad array of recent studies, CDOM and FDOM parameters may be used to examine DOM composition (i.e., source) and assess dissolved organic carbon (DOC) concentration (McKnight et al., 2001; Spencer et al., 2012; Stedmon et al., 2003; Weishaar et al., 2003). Furthermore, FDOM parameters have been used to identify the presence of several types of contaminants including polycyclic aromatic hydrocarbons and fluorescent brightening and whitening agents present in wastewater and sewage-impacted surface and groundwater (Baker, 2001; Birdwell & Engel, 2009; Hudson et al., 2007). Due to the lack of photosynthesis and photodegradation in karst aquifers, the DOM found in these environments is expected to reflect allochthonous and anthropogenic inputs or be a product of chemolithotrophic primary production or microbial degradation with distinct CDOM and FDOM characteristics (Baker & Genty, 1999; Baker & Lamont-Black, 2001; Birdwell & Engel, 2009). Therefore, examination of CDOM and FDOM parameters found throughout a conduit and vent ecosystem may be utilized to link DOM back to its source, and assess the drivers of DOM at a spring vent.

The aim of this study was to evaluate the dominant sources of DOM at the vent of a major spring (Wakulla Springs) by relating DOC concentration and DOM composition in the major conduits that feed into the spring vent, to the evolved signature from the vent. The modification of this signature from the vent was then further examined to the closest downstream hydrology gauging station to allow for relationships between discharge and DOM characteristics to be assessed. The study was conducted over 1 year to encompass seasonal variability in hydrology as well as to examine impacts on seasonality of the DOM sources feeding into the conduit and vent system. The samples were taken from major conduits draining a range of land cover, from those dominated by forested areas to those predominantly encompassing urban regions, and encapsulated all the major conduits that feed into the Wakulla Springs vent. Ultimately, our goal was to determine if CDOM and FDOM parameters can delineate the different sources of DOM feeding into the Wakulla Springs vent and determine which sources are responsible for the colored water that has become increasingly common at the vent in recent decades (Florida Geological Survey Special Publication 58, 2005).

2. Methods

2.1. Study Site

A spring with an average discharge of 2.8 m^3/s or greater is categorized as a magnitude one spring. Wakulla Springs is the largest and deepest freshwater spring in the world with an average discharge of 19.8 m^3/s flowing from a 30.5-m diameter vent (Xu et al., 2015). Wakulla Springs vent is the headwaters for the Wakulla River and flows 10 km before entering the St. Marks River, which continues into the Gulf of Mexico. Wakulla Springs is located in north Florida and is part of the Woodville Karst Plain (WKP). Within the Wakulla springshed, major features are the Apalachicola National Forest in the western region and the City of Tallahassee (population ~ 187,500) to the north of the spring vent (Figure 1). Land use within the springshed encompasses forested land (43%), wetlands and lakes (23%), agricultural and pasture lands (~21%), and urban/commercial developments (~13%) (Florida Springs Institute, 2014). Within the WKP, the Upper Floridan Aquifer has 59.5 km of human navigable conduits and is characterized by highly porous quartz sand, along with some clay and silt (Xu et al., 2016). Through dye traces and cave expeditions, several major conduits that discharge at Wakulla Springs have been identified and located (Figure 1b). From Wakulla Springs vent (sample site VIII), the conduit system runs southwest with conduits A and K flowing from the Apalachicola National Forest; sample sites V–

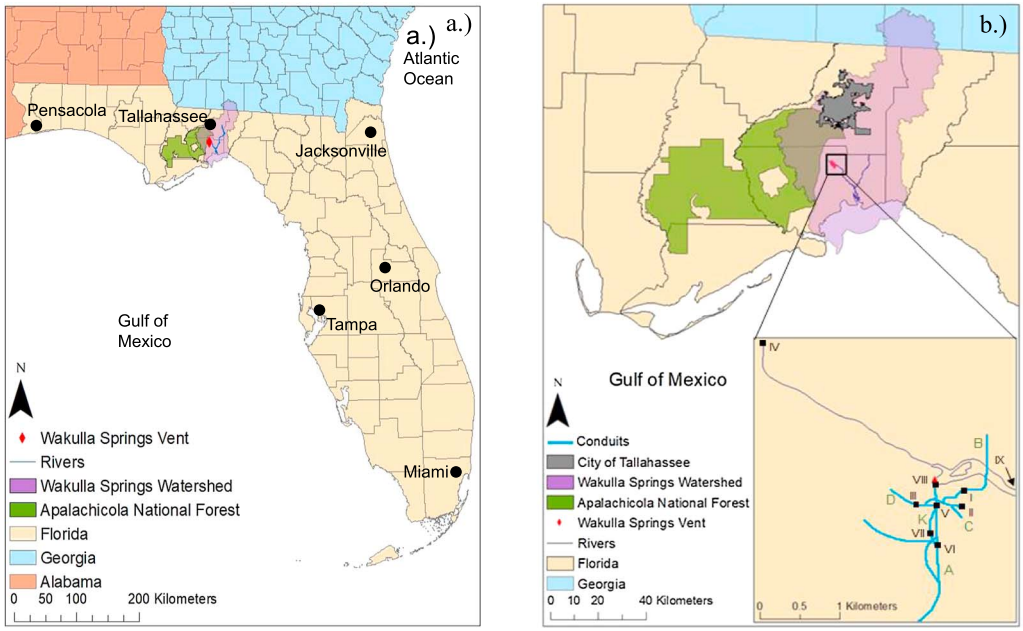

Figure 1. (a) Map of study area within the southeastern United States of America. (b) Map of the nine sampling locations encompassing the major conduits and vent of Wakulla Springs.

VII come from these conduits (Figure 1b). Conduits B and D run north-south and converge into conduit C before discharging at Wakulla Springs vent; sample sites I–III come from these conduits (Figure 1b). Sally Ward, sample site IV, is a connecting spring located 1 km northwest of the main spring and enters the Wakulla River 183 m downstream from its source (Figure 1b). Sample site IX is taken from a downstream bridge approximately 3 km from the Wakulla Springs vent (Figure 1b).

2.2. Sample Collection

Samples were collected biweekly from August 2015 to August 2016, with a total of 26 sampling events. Nine samples were collected at every sampling event including sampling from three wells, with two lines in each well feeding into separate conduits that lie ~100 m underground: the Sally Ward Spring, the vent of the Wakulla Springs system, and a downstream location 3 km from the vent that has continuous discharge data (gauge 02327022, United States Geological Survey, 2018). Samples collected from the wells, Sally Ward Spring, and Wakulla Springs vent were pumped and field filtered through 0.7-μm Whatman glass fiber filters (GF/F, precombusted at 450 °C) using a peristaltic pump after purging the well line. Surface water was collected from the most downstream location (site IX) by sampling from the thalweg and was subsequently filtered (GF/F, precombusted at 450 °C) back in the laboratory within 1 hr of collection. Samples were collected in acid-washed polycarbonate bottles (1 L), stored in the dark on ice during transportation, and then in a refrigerator (450 °C) back in the laboratory until analysis (typically within 24–48 hr).

2.3. DOC Concentration and Optical Properties

Samples for DOC concentration were acidified to pH 2 and stored in a refrigerator (4 °C) until analysis by high-temperature combustion on a Shimadzu TOC-L CPH using the nonpurgeable organic carbon method (sparged at 75 mL/min for 8 min), within 2 weeks following collection. DOC was calculated as the mean of between three and five injections using a six-point standard curve using established protocols (Mann et al., 2012), and the coefficient of variance was always $<2\%$.

Samples with low CDOM absorbance (≤ 0.02 at 350 nm) were measured using a 10-cm cuvette on an Agilent 8453 ultraviolet-visible spectrophotometer, whereas samples above this absorbance threshold were analyzed in a 1-cm cuvette on a Horiba Aqualog-UV-800-C. Absorbance spectra were measured from 230 to 800 nm and corrected for a small offset either due to long-term baseline drift or derived from glass fiber

particles during filtration (Blough et al., 1993) by subtracting the mean absorbance measured between 750 and 800 nm. Two spectral slopes were calculated at 275–295 and 350–400 nm ($S_{275-295}$ and $S_{350-400}$, respectively), and the spectral slope ratio (S_R) was then calculated by dividing the former by the latter (Helms et al., 2008). The CDOM absorption ratio at 250 to 365 nm was calculated (a_{250}:a_{365}), and specific ultraviolet absorbance ($SUVA_{254}$) was calculated by dividing the decadic absorption coefficient at 254 nm by DOC concentration (Fellman et al., 2009; Weishaar et al., 2003).

Fluorescence properties of FDOM were determined using a Horiba Aqualog-UV-800-C. The excitation emission matrices (EEMs) were generated in a 1-cm cuvette at varying integration times (1–10 s) to maximize the signal-to-noise ratio based on absorbance values. The EEMs were obtained at excitation (ex) 250–600 nm and at emission (em) 250–600 nm with 5- and 2-nm intervals, respectively, and the EEMs were corrected for lamp intensity (Cory et al., 2010), inner filter effects (Kothawala et al., 2013), and normalized to Raman units (Stedmon et al., 2003). All corrections were performed using the FDOMcorr toolbox version 1.6 (Murphy, 2011). EEMs were analyzed with parallel factor analysis (PARAFAC) using the procedure described in Murphy et al. (2013). The model was validated using core consistency diagnostics and a split-half validation procedure. The PARAFAC model revealed two humic-like components (C1 ex/em: <260, 355/449; C2 ex/em: 385, 265/509), two microbial humic-like components (C3 ex/em: <260, 310/412; C5 ex/em: 335, 290/393), and two protein-like components (tryptophan-like C4, ex/em: 295/352 and tryosine-like C6, ex/em: 275/304; supporting information Figure S1). All components were matched with previous studies according to Openfluor (www.openfluor.org; supporting information Table S1). Furthermore, the fluorescence index (FI, Cory et al., 2010), humification index (HIX, Ohno, 2002; Zsolnay et al., 1999), and autotrophic productivity index (BIX, Huguet et al., 2009) were calculated. FI was calculated from the emission wavelengths at 470 and 520 nm, obtained at excitation 370 nm (Cory & McKight, 2005). HIX was calculated using the area under the emission spectra 435–480 nm divided by the peak area 300–345 + 435–480 nm, at excitation 254 nm (Ohno, 2002). BIX was calculated from the emission intensity of 380 and 430 nm, obtained at excitation 310 nm (Wang et al., 2014).

2.4. Statistical Analyses

All statistical analyses were done in JMP® Pro, Version 13.1. Differences in variables among site types were evaluated using analysis of variance. Homoskedasticity was tested using Bartlett's test for equal variances between site types, and all variables exhibited heteroskedasticity of variance across site types with p value < 0.0001. Thus, the difference among groups was determined using a Kruskall-Wallace χ^2 test. Pairwise comparisons were evaluated using the nonparametric Wilcoxon method. Principal component analysis (PCA) was used to assess the relationships in optical properties between site types across seasons and to identify optical properties that were most strongly associated with each site type. PCA was assessed on log-transformed variables including DOC concentration, absorbance and fluorescence indices, and the percent contribution of each PARAFAC component.

3. Results

3.1. DOC Concentration

The mean DOC concentrations at all sample sites ranged from 0.38 to 2.57 mg/L (Table 1 and Figure 2a). At sample sites I–IV, DOC concentrations were consistently low with a mean range of 0.38–0.52 mg/L. At sites V–IX, DOC concentrations were at least 3 times higher in comparison to sites I–IV with a mean range of 1.85–2.57 mg/L (Table 1 and Figure 2a). The low observed DOC concentrations at sites I–IV are highly comparable to data from pristine aquifers globally and groundwater studies in South Carolina (Regan et al., 2017; Shen et al., 2015). The higher DOC concentrations at sites V–IX also show a greater range in DOC concentrations particularly at sites V–VII ranging up to 6.69 mg/L (Figure 2a), with concentrations highly comparable to most U.S. rivers, as well as polluted aquifers (Regan et al., 2017; Spencer et al., 2012). Both the mean DOC values and the range of DOC concentrations at sites V–VII are strikingly similar to the DOC concentrations observed at the vent (site VIII) and downstream bridge (site IX, Table 1 and Figure 2a). However, it is noteworthy that the DOC concentrations at the vent are systematically lower than observed in sites V–VII, reflecting the mixing of water from the lower DOC conduits (I–III) diluting these higher DOC conduits prior to discharge from the vent.

Table 1
Mean and Standard Deviations of Dissolved Organic Carbon Concentration and Chromophoric and Fluorescent Dissolved Organic Matter Parameters for Sample Sites

Sample sites	DOC (mg/L)	a_{254} (m^{-1})	a_{350} (m^{-1})	a_{440} (m^{-1})	$SUVA_{254}$ (L·mg C^{-1}·m^{-1})	a_{250}:a_{365}	$S_{275-295}$ ($\times10^{-3}$ nm^{-1})	$S_{350-400}$ ($\times10^{-3}$ nm^{-1})	S_R	FI	HIX	BIX
I	0.52 (0.64)	0.83 (0.71)	0.33 (0.61)	0.35 (0.61)	2.32 (1.56)	7.04 (4.21)	14.86 (5.21)	22.71 (21.19)	1.16 (1.36)	1.78 (0.15)	6.20 (5.18)	0.75 (0.34)
II	0.51 (0.58)	0.87 (0.52)	0.25 (0.32)	0.14 (0.27)	2.45 (1.12)	9.38 (8.84)	16.01 (3.60)	22.04 (15.99)	0.93 (0.60)	1.67 (0.07)	8.18 (10.85)	0.90 (0.30)
III	0.39 (0.42)	0.56 (0.23)	0.13 (0.10)	0.09 (0.09)	2.00 (1.04)	9.21 (5.54)	18.96 (7.10)	23.86 (17.34)	1.11 (0.83)	1.76 (0.11)	5.98 (5.77)	0.92 (0.33)
IV	0.38 (0.53)	0.63 (0.34)	0.17 (0.29)	0.19 (0.37)	2.30 (1.05)	8.63 (4.89)	16.23 (4.57)	28.64 (28.17)	0.96 (0.74)	1.74 (0.10)	13.54 (24.93)	0.88 (0.43)
V	2.57 (1.66)	10.67 (7.90)	3.43 (2.64)	0.89 (0.74)	4.00 (0.82)	4.19 (0.47)	12.39 (1.05)	16.08 (3.16)	0.78 (0.08)	1.44 (0.04)	21.54 (11.71)	0.51 (0.08)
VI	2.42 (1.55)	10.10 (7.30)	3.22 (2.46)	0.80 (0.71)	4.04 (0.87)	4.26 (0.44)	12.67 (1.18)	16.62 (2.75)	0.77 (0.06)	1.44 (0.04)	19.53 (9.90)	0.51 (0.05)
VII	2.22 (1.56)	8.97 (6.78)	2.68 (2.19)	0.60 (0.61)	3.98 (0.67)	4.65 (0.49)	13.40 (1.14)	18.33 (3.19)	0.74 (0.07)	1.48 (0.03)	17.79 (6.21)	0.53 (0.05)
VIII	2.02 (1.31)	7.51 (6.04)	2.39 (2.04)	0.59 (0.58)	3.73 (1.26)	4.37 (0.66)	12.99 (1.59)	17.20 (3.22)	0.76 (0.07)	1.46 (0.05)	20.75 (18.33)	0.53 (0.05)
IX	1.85 (1.10)	7.53 (5.42)	2.42 (1.79)	0.66 (0.51)	3.90 (0.81)	4.14 (0.60)	13.05 (1.35)	15.26 (3.15)	0.89 (0.19)	1.46 (0.04)	10.70 (7.88)	0.60 (0.17)

Note. DOC = dissolved organic carbon; FI = fluorescence index; BIX = autotrophic productivity index; HIX = humification index.

3.2. CDOM Parameters

CDOM absorbance for commonly utilized wavelengths (e.g., a_{254}, a_{350}, and a_{440}) exhibited similar trends across wavelengths at all sample sites (Table 1). For example, the mean a_{350} values at all sample sites ranged from 0.13 to 3.43 m^{-1} (Table 1 and Figure 2b). At sample sites I–IV, a_{350} values were consistently low with a mean range of 0.13–0.33 m^{-1}. These low values are indicative of extremely CDOM poor water and are comparable to values from marine waters and other groundwater-dominated systems (Arellano & Coble, 2015; Guéguen et al., 2014; Massicotte et al., 2017; Para et al., 2010). Values for a_{350} at sample sites V–IX were higher in comparison to sites I–IV with a mean range of 2.39–3.43 m^{-1} (Table 1 and Figure 2b). These mean values for a_{350} at sample sites V–IX were thus comparable to data reported in major Arctic rivers during groundwater-dominated under-ice flows in the winter months (Mann et al., 2012; Spencer, Aiken, et al., 2009; Stedmon, et al., 2011). The higher values observed for a_{350} at samples sites V–IX (up to 9.52 m^{-1}, Figure 2b) are similar to typical a_{350} values reported in a broad range of global rivers (Massicotte et al., 2017; Spencer et al., 2012). As noted above with respect to DOC concentrations, a_{350} values at sites V–VII are highly comparable to a_{350} values at sites VIII (vent) and IX (the downstream bridge, Table 1 and Figure 2b).

The mean $SUVA_{254}$ values at all sample sites ranged from 2.00 to 4.04 L·mg C^{-1}·m^{-1} (Table 1 and Figure 3a). Using ^{13}C nuclear magnetic resonance, $SUVA_{254}$ values have been positively correlated to the percent aromaticity of DOM (Weishaar et al., 2003). At sample sites I–IV, $SUVA_{254}$ values stayed consistently low with a mean range of 2.00–2.45 L·mg C^{-1}·m^{-1}. At sample sites V–IX, $SUVA_{254}$ values were relatively higher in comparison, with a mean range of 3.73–4.04 L·mg C^{-1}·m^{-1} (Table 1 and Figure 3a). The lower values observed for $SUVA_{254}$ at sites I–IV are comparable to rivers with significant autochthonous inputs, such as the Colorado River (1.67 L·mg C^{-1}·m^{-1}), the Rio Grande River (2.03 L·mg C^{-1}·m^{-1}), and the Columbia River (2.62 L·mg C^{-1}·m^{-1}, Spencer et al., 2012), as well as groundwater studies in South Carolina (1.54 L·mg C^{-1}·m^{-1}, Shen et al., 2015). The higher $SUVA_{254}$ values observed at sites V–IX were comparable to U.S. rivers with major allochthonous inputs, for example, blackwater rivers (3.40–4.50 L·mg C^{-1}·m^{-1}, Spencer et al., 2008, 2012). The vent (site VIII) and downstream bridge (site IX) mean values of $SUVA_{254}$ were similar too but consistently slightly lower than observed for sites V–VII, suggesting mixing with lower $SUVA_{254}$ water from conduit sites I–III (Table 1 and Figure 3a).

The a_{250}:a_{365} ratio has been linked to the aromatic content and molecular size of DOM, with increasing values indicating a decrease in aromaticity and molecular size (Peuravuori & Pihlaja, 1997). The mean a_{250}:a_{365} values at all sites ranged from 4.14 to 9.38 (Table 1). At sample sites I–IV, a_{250}:a_{365} values were high with a mean range of 7.04–9.38. At sample sites V–IX, a_{250}:a_{365} values were much lower in comparison with a mean range of 4.14–4.65. The lowest mean a_{250}:a_{365} values are comparable to aquatic ecosystems with significant blackwater inputs, such as the St. Marys River (4.20), the Mobile River (4.80, Spencer et al., 2012), and the Great Dismal Swamp (4.57–4.64, Helms et al., 2008). The highest mean a_{250}:a_{365} values are comparable to the St. Lawrence River (9.65, Spencer

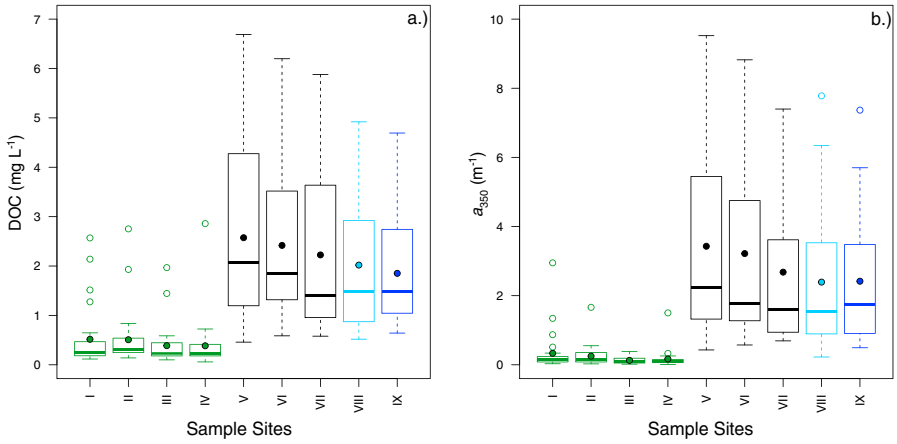

Figure 2. (a) Box plots showing the range of DOC concentrations at each site throughout the year. (b) Box plots showing the range of a_{350} values at each site throughout the year. Green boxes represent clear water sites, black boxes represent forested sites, light blue boxes represent the Wakulla Springs vent, and dark blue boxes represent the downstream bridge. Filled in circles represent mean values, and horizontal lines represent medians for each sample sites. DOC = dissolved organic carbon.

et al., 2012) and coastal waters in the Georgia Bight (8.70, Helms et al., 2008). The vent (site VIII) and downstream bridge (site IX) reflected similar values to sites V–VII, indicating that these sites are dominant drivers of a_{250}:a_{365} found at sites VIII and IX.

The spectral slope parameter (S) is frequently used to evaluate the quality of CDOM and has been observed to vary with CDOM source (Blough & Del, 2002). Steeper S values are related to a decrease in molecular weight and aromaticity of DOM (Blough & Green, 1995; Helms et al., 2008). The range of wavelengths 275–295 nm ($S_{275-295}$) and 350–400 nm ($S_{350-400}$) has been historically chosen as they have been observed to show the greatest variation in aquatic ecosystems (Helms et al., 2008; Spencer et al., 2012). The mean $S_{275-295}$ values at all samples sites ranged from 12.39 to 18.96 × 10^{-3} nm^{-1} (Table 1 and Figure 3b). At sample sites I–IV, $S_{275-295}$ values were relatively high with a mean range of 14.86–18.96 × 10^{-3} nm^{-1} and also had a much greater range of values in comparison to sites V–IX (Table 1 and Figure 3b). At sample sites V–IX, $S_{275-295}$ values were much lower in comparison with a mean range of 12.39–13.40 × 10^{-3} nm^{-1}. The shallowest mean $S_{275-295}$ values are comparable to allochthonous-dominated waters, for example, the St. Marys River (12.47 × 10^{-3} nm^{-1}) and Lookout Creek (13.19 × 10^{-3} nm^{-1}, Spencer et al., 2012). The steepest mean $S_{275-295}$ values are similar to sites dominated by autochthonous inputs, for example, the Rio Grande (19.80 × 10^{-3} nm^{-1}) and the Columbia River (16.33 × 10^{-3} nm^{-1}, Spencer et al., 2012), as well as the Chesapeake Bay (17.40 × 10^{-3} nm^{-1}, Helms et al., 2008). The mean $S_{350-400}$ values at all samples sites ranged

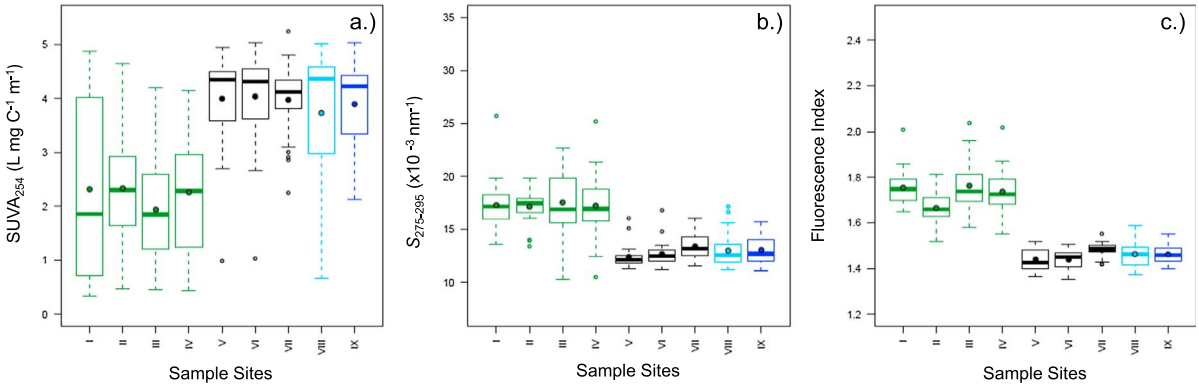

Figure 3. (a) Box plots showing the range of $SUVA_{254}$ at each site throughout the year. (b) Box plots showing the range of $S_{275-295}$ at each site throughout the year. (c) Box plots showing the range of fluorescence index at each site throughout the year. Green boxes represent clear water sites, black boxes represent forested sites, light blue boxes represent the Wakulla Springs vent, and dark blue boxes represent the downstream bridge. Filled in circles represent mean values, and horizontal lines represent medians for each sample sites. $SUVA_{254}$ = specific ultraviolet absorbance.

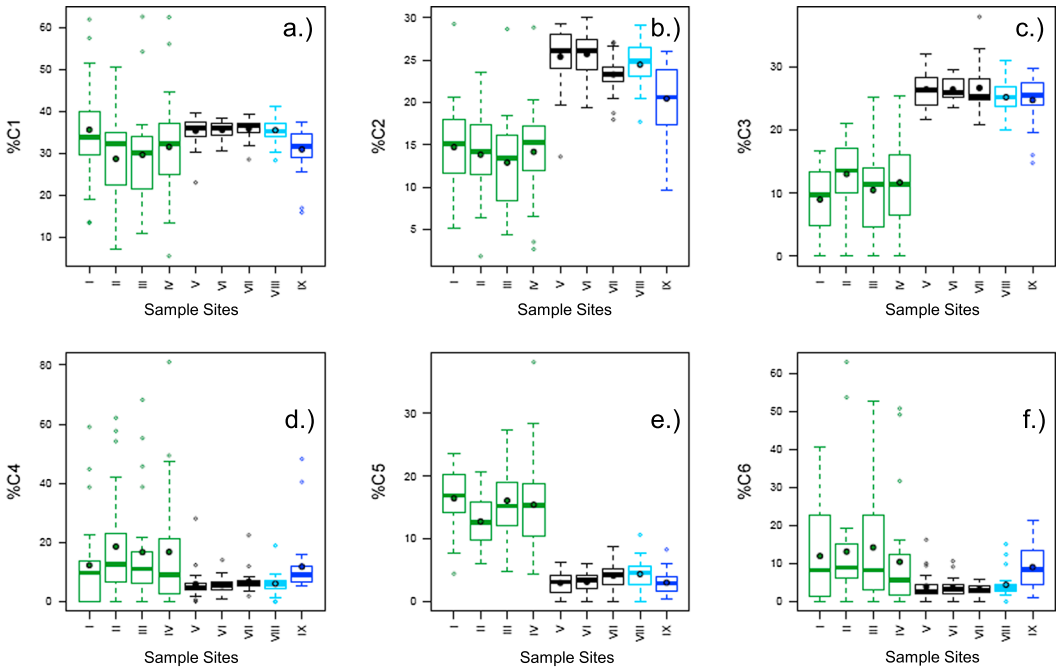

Figure 4. (a) Box plots showing the percent of each component at each site throughout the year. Green boxes represent clear water sites, black boxes represent forested sites, light blue boxes represent the Wakulla Springs vent, and dark blue boxes represent the downstream bridge. Filled in circles represent mean values, and horizontal lines represent medians for each sample sites.

from 15.26 to 28.64 × 10^{-3} nm^{-1} (Table 1). At sample sites I–IV, $S_{350–400}$ values were elevated with a mean range of 22.04–28.64 × 10^{-3} nm^{-1}. At sample sites V–IX, $S_{350–400}$ values were relatively shallow in comparison with a mean range of 15.26–18.33 × 10^{-3} nm^{-1}. The shallowest mean $S_{350–400}$ values are comparable to aquatic ecosystems with high allochthonous inputs such as the Congo River (15.21 × 10^{-3} nm^{-1}, Spencer, Stubbins, et al., 2009) and the Evergreen River (15.97 × 10^{-3} nm^{-1}, Spencer et al., 2012). The steepest mean $S_{350–400}$ values are comparable to coastal waters (18.00–19.00 × 10^{-3} nm^{-1}, Shank & Evans, 2011) and prairie lakes (22.41 × 10^{-3} nm^{-1}, Osburn et al., 2011). The vent (site VIII) and downstream bridge (site IX) mean values and ranges for both $S_{275–295}$ and $S_{350–400}$ were more comparable to sites V–VII than sites I–IV.

The spectral slope ratio (S_R, $S_{275–295}$:$S_{350–400}$) has also been used to characterize CDOM in natural waters, with lower relative values indicative of DOM with higher molecular weight and greater aromaticity (Helms et al., 2008; Osburn et al., 2011; Spencer et al., 2010). The mean S_R values at all sample sites ranged from 0.74 to 1.16 (Table 1). At sample sites I–IV, the mean S_R values ranged from 0.93 to 1.16, higher than the mean S_R values at sample sites V–IX (0.74–0.89). Lower mean S_R values from sites V–IX are similar to the blackwater St. Marys River (0.75, Spencer et al., 2012) and data from major Arctic rivers (0.79) when they receive significant vascular plant inputs at the peak of spring freshet (Spencer, Aiken, et al., 2009; Stedmon, et al., 2011). The highest S_R values at sites I–IV are comparable to the autochthonous-dominated St. Lawrence River (1.23, Spencer et al., 2012) and approaching values reported for coastal marine waters in the northern Gulf of Mexico (1.20–1.40, Shank & Evans, 2011). The S_R values observed at the vent (site VIII) and downstream bridge (site IX) are similar to S_R values reported for sites V–VII.

3.3. Fluorescent Dissolved Organic Matter Parameters

The FI was derived to assess the relative contribution of microbial-derived DOM versus higher plant-derived DOM, with lower values indicative of terrestrial-sourced DOM (McKnight et al., 2001). The mean FI values at all sample sites ranged from 1.44 to 1.78 (Table 1 and Figure 3c). At sample sites I–IV, the mean FI values were high with a range of 1.67–1.78. These high FI values are comparable to those reported in microbially dominated end-members, such as Pony Lake in Antarctica (1.7, McKnight et al., 2001), and samples taken at baseflow in the Juruena River Basin (1.6, Johnson et al., 2011). In sample sites V–IX, the mean FI values were much

Table 2
Results From Rank-Based ANOVAs Using the Kruskall-Wallis Test

Variable	DOC (mg/L)	a_{350} (m^{-1})	$SUVA_{254}$ (L mgC^{-1} m^{-1})	a_{250}: a_{365}	$S_{275-295}$ ($\times10^{-3}$ nm^{-1})	FI	HIX	BIX	% C1	% C2	% C3	% C4	% C5	% C6
χ^2 (Kruskal-Wallis test)	138	153	90	52	52	169	102	127	33	138	160	30	163	42
Clear	A	A	A	A	A	A	A	A	A	A	A	A	A	A
Forested	B	B	B	B	B	B	B	B	B	B	B	B	B	B
Vent	B	B	B	B	B	B	B	BC	B	B	B	B	B	B
Bridge	B	B	B	B	B	B	C	C	A	C	B	A	B	A

Note. All variables were heteroskedastic with a p value < 0.0001. χ^2 tests had 3 degrees of freedom. Variables listed in table were significant χ^2 at a level of p value < 0.0001. There were no differences in $S_{350-400}$ and S_R among site types, and therefore, they were not included in the table. Pairwise comparisons are represented using a connecting letters report. Site types not connected by the same letter are significantly different, as determined by nonparametric pairwise comparisons using the Wilcoxon method. P value < 0.001 for all pairwise comparisons, except for differences between vent and clear waters in %C1, %C4, and %C6 (p value < 0.01). ANOVA = analysis of variance; DOC = dissolved organic carbon; FI = fluorescence index; BIX = autotrophic productivity index; HIX = humification index.

lower and occupied a narrow range from 1.44 to 1.48 (Table 1 and Figure 3c). These low mean FI values are comparable to vascular plant-dominated end-members, such as the Ogeechee and Missouri Rivers (1.4–1.5, McKnight et al., 2001), and tributaries of the Juruena River with major terrestrial inputs (1.5, Johnson et al., 2011).

Other fluorescence indices (HIX and BIX) were used to examine degradation history and sources of DOM throughout the conduit and vent ecosystem. The HIX increases with greater humification of source material (Ohno, 2002), while BIX values decrease with increasing contributions from allochthonous DOM (Huguet et al., 2009). Sites I–IV had lower mean HIX values and higher BIX mean values compared to sites V–IX (Table 1). Comparable data to the mean ranges of HIX and BIX found at sites I–IV (5.98–13.54 and 0.75–0.92, respectively, Table 1) have been observed in previous studies in samples dominated by autochthonous DOM (Birdwell & Engel, 2010; Huguet et al., 2009; Ohno, 2002). Sites V–IX showed the opposite trend of high HIX mean values (10.70–21.54) and low BIX mean values (0.51–0.60, Table 1). Similar values to the means reported here for sites V–IX have been observed in past studies highlighting terrestrial DOM inputs (Bianchi et al., 2011; Kothawala et al., 2012). As described for a number of other parameters above, the vent (site VIII) had similar values for FI, HIX, and BIX to sites V–VII emphasizing the influence of these conduits on the DOM exported from the Wakulla Springs vent.

The six components found in the PARAFAC model (supporting information Figure S1) exhibited clear variability in terms of intensities and relative contributions between sites (Figure 4 and supporting information Figure S2). Here we focus on the relative contribution of PARAFAC components (%C) as this has been shown to be a useful metric with respect to assessing DOM quality independent of DOC concentration (Fellman et al., 2009; Kothawala et al., 2014). Overall, the percent contributions from C1 (humic-like component), C2

Table 3
Relationship Between DOC and CDOM Absorption Coefficients (a_{254}, a_{350}, and a_{440})

Absorbance (m^{-1})	Site	n	r^2	P	Slope	Standard error	Int.	Standard error
a_{254}	Clear	101	0.078	0.0048	0.26	0.088	0.61	0.06
	Forested	77	0.913	<0.0001	4.39	0.156	−0.69	0.45
	Vent	26	0.642	<0.0001	3.68	0.561	0.08	1.34
	Bridge	26	0.966	<0.0001	4.83	0.185	−1.32	0.40
a_{350}	Clear	99	0.010	0.3166	0.07	0.070	0.19	0.05
	Forested	77	0.905	<0.0001	1.46	0.055	−0.41	0.16
	Vent	26	0.636	<0.0001	1.24	0.192	−0.11	0.46
	Bridge	26	0.951	<0.0001	1.59	0.074	−0.52	0.16
a_{440}	Clear	60	0.002	0.7186	0.03	0.094	0.18	0.07
	Forested	77	0.848	<0.0001	0.40	0.020	−0.20	0.06
	Vent	26	0.596	<0.0001	0.34	0.058	−0.10	0.14
	Bridge	26	0.793	<0.0001	0.42	0.043	−0.11	0.09

Note. DOC = dissolved organic carbon; CDOM = chromophoric dissolved organic matter.

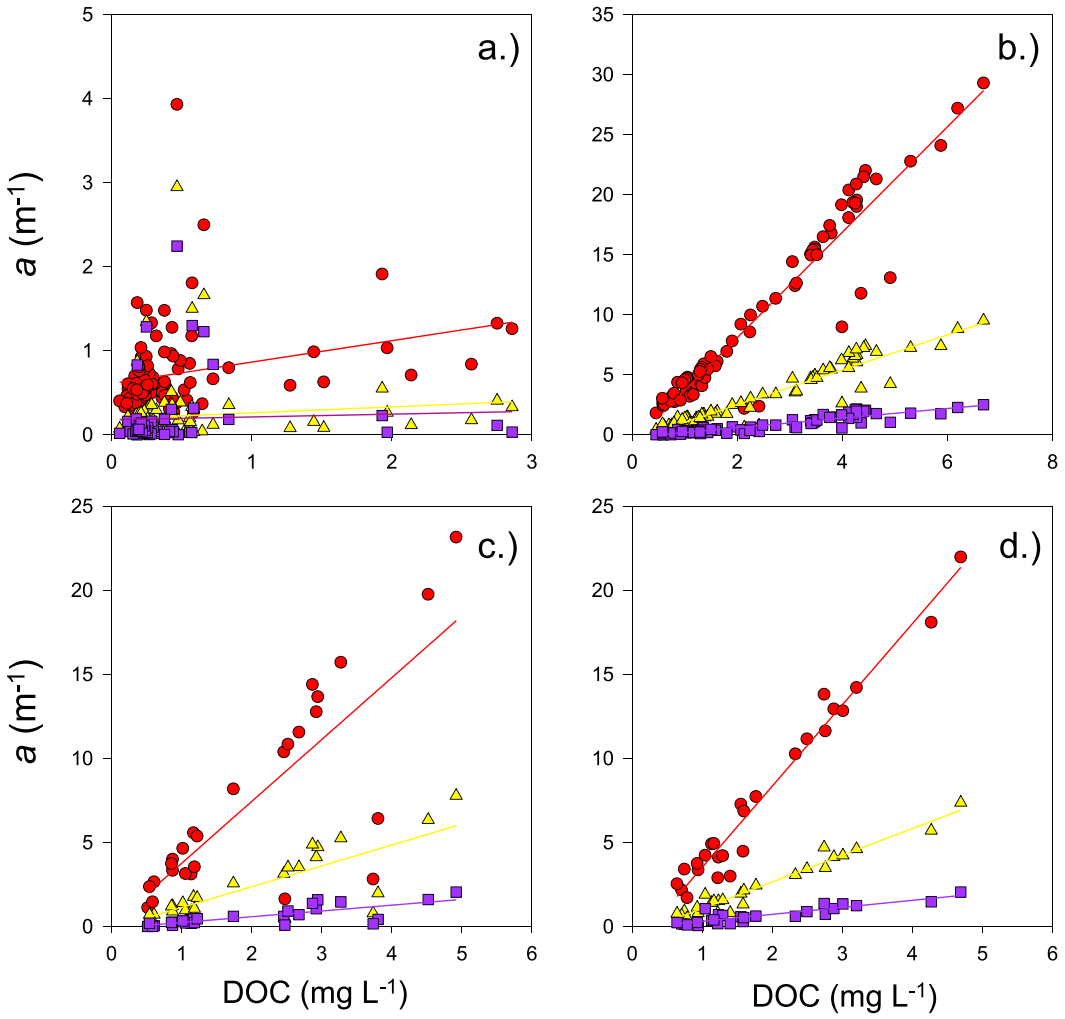

Figure 5. Absorbance values at clear water sites (a), forested sites (b), the vent (c), and the downstream bridge (d) versus DOC throughout the year. Red circles represent a_{254}, yellow triangles represent a_{350}, and purple squares represent a_{440}. DOC = dissolved organic carbon.

(humic-like component), and C3 (microbial humic-like component) show similar trends with relatively greater proportions assigned to sites V–IX in comparison to sites I–IV (Figures 4a–4c) (supporting information Table S2). Conversely, with respect to %C4 (protein-like component), %C5 (microbial humic-like component), and %C6 (protein-like component) sites I–IV exhibit greater contributions in comparison to sites V–IX (Figures 4d–4f and supporting information Table S2). With respect to all six components the vent and downstream bridge (sites VIII and IX, respectively) are always highly comparable to the means and ranges reported for the conduits V–VII (supporting information Table S2). Despite the overall similarities between sites V–VII and VIII and IX, for components C1–C3, the vent and bridge sites show a slight decrease in relative contribution in comparison to sites V–VII and conversely a slight increase in relative contribution when examining components C4–C6 (Figure 4). This emphasizes that although the conduits V–VII might be driving the DOM signature at the vent and subsequently downstream, mixing with water from the conduits (I–III) is apparent in the FDOM signature at the vent.

4. Discussion

4.1. Linking DOM From Conduits to the Vent at Wakulla Springs

On examination of the sample sites from within the conduits and Sally Ward Spring (sites I–VII), a distinct separation occurs between sites I–IV and V–VII. Sites I–IV are characterized by low DOC concentrations, low

Table 4
Relationship Between Each Component Versus DOC at Clear Water Sites, Forested Sites, the Vent, and Downstream Bridge

Component	Site	$_r2$	P	Slope	Standard error	Int.	Standard error
1	Clear	0.101	0.001	0.04	0.013	0.16	0.01
	Forested	0.885	<0.0001	0.49	0.020	0.11	0.06
	Vent	0.648	<0.0001	0.41	0.062	0.05	0.15
	Bridge	0.907	<0.0001	0.51	0.033	−0.08	0.07
2	Clear	0.204	<0.0001	0.02	0.004	0.07	0.01
	Forested	0.908	<0.0001	0.37	0.013	0.04	0.04
	Vent	0.660	<0.0001	0.32	0.047	−0.01	0.11
	Bridge	0.928	<0.0001	0.37	0.021	−0.10	0.05
3	Clear	0.039	0.05	0.02	0.008	0.06	0.01
	Forested	0.861	<0.0001	0.32	0.015	0.16	0.04
	Vent	0.650	<0.0001	0.29	0.043	0.04	0.10
	Bridge	0.890	<0.0001	0.37	0.027	−0.01	0.06
4	Clear	0.003	0.59	0.02	0.044	0.13	0.03
	Forested	0.284	<0.0001	0.07	0.012	0.06	0.03
	Vent	0.269	0.01	0.07	0.025	0.02	0.06
	Bridge	0.005	0.74	0.02	0.054	0.26	0.12
5	Clear	0.242	<0.0001	0.04	0.006	0.07	0.01
	Forested	0.400	<0.001	0.04	0.005	0.02	0.01
	Vent	0.026	0.43	−0.28	0.348	0.11	0.03
	Bridge	0.151	0.05	0.02	0.008	0.04	0.02
6	Clear	0.308	<0.0001	0.28	0.042	0.00	0.03
	Forested	0.265	<0.0001	0.04	0.008	0.02	0.02
	Vent	0.192	0.03	0.04	0.017	0.03	0.04
	Bridge	0.020	0.49	0.02	0.033	0.16	0.07

Note. DOC = dissolved organic carbon.

CDOM values, and optical parameters indicative of low molecular weight and low aromaticity DOM, which has greater relative protein-like fluorescence contribution than sites V–VII (Table 1 and Figures 2–4). These sites (I–IV) thus appear dominated by DOM highly comparable to that observed in previous groundwater studies (Chen et al., 2010; Shank & Evans, 2011; Shen et al., 2015; Spencer et al., 2012), and in this study they are labeled clear water. The conduits feeding into sites I–IV bring water from the WKP that is composed of highly karstified, unconsolidated and porous sands and limestone and lead to exceptionally clear water low in organic matter content (Xu et al., 2016). These sites also receive inputs from surface runoff associated with the city of Tallahassee as well as potential anthropogenic contamination sources (e.g., a wastewater facility including a spray field and a landfill facility) within this portion of the springshed (Berndt, 1990; Xu et al., 2016).

Conversely, sites V–VII are characterized by comparatively high DOC concentrations, high CDOM values, optical parameters indicative of a dominance of high molecular weight, and aromatic DOM, as well as a greater relative contribution of humic-like fluorescence, particularly from C2 that has the most red-shifted fluorescence emission maxima of all identified components (supporting information Figure S1, Table 1, and Figures 2–4). Such red shifted fluorophores with broad emission maxima are typically derived from vascular plant and soil organic matter sources, are aromatic in nature and highly conjugated, and represent the higher molecular weight fraction of DOM (Coble et al., 1998; Fellman et al., 2010). These sites (V–VII) predominantly drain parts of the Apalachicola National Forest and appear to contain allochthonous DOM. The general characteristics with respect to DOC concentrations and DOM quality of sites V–VII are highly comparable to previous studies examining aquatic environments in blackwater, swamp, and forested systems (Chen et al., 2010; Helms et al., 2008; Spencer, Stubbins, et al., 2009; Stedmon, et al., 2011), and in this study they are labeled forested to reflect their source in the Apalachicola National Forest. With respect to both DOC concentration and DOM optical parameters (Tables 1 and 2 and Figures 2–4) it is apparent that sites VIII and IX are highly comparable to sites V–VII. This is particularly apparent when comparing the forested sites (V–VII) to the vent (VIII), as Table 2 highlights no significant difference between DOC concentrations and all the measured DOM optical parameters between these sites. However, for most parameters the dilution with clear water DOM from sites I–III in the conduit system and then from site IV (Sally Ward Spring) downstream from the

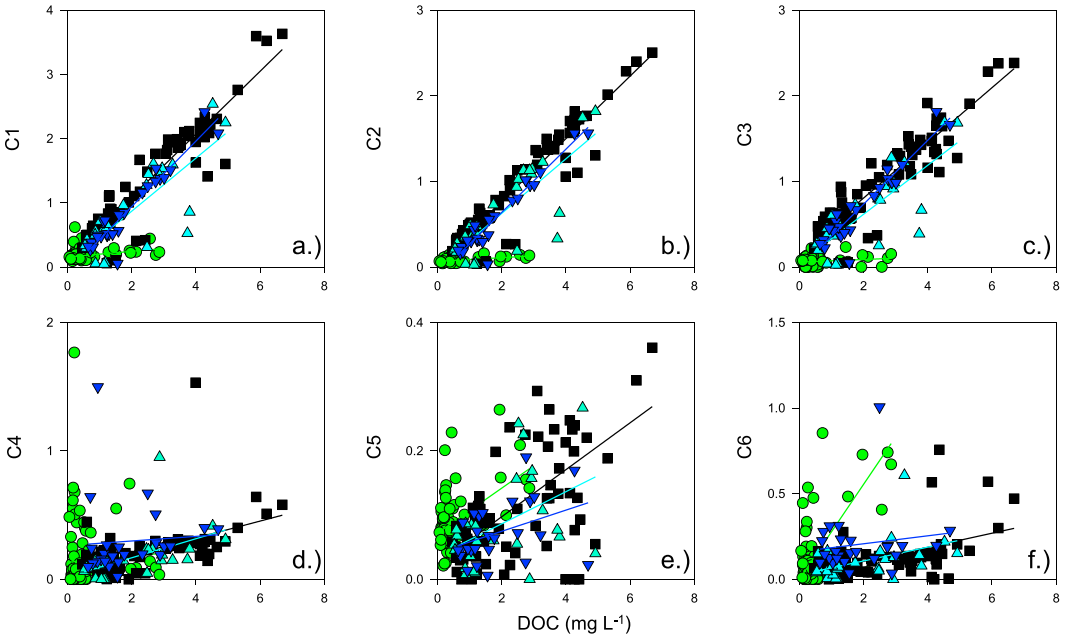

Figure 6. PARAFAC components 1–6 (a–f) versus DOC at each site throughout the year. Green circles represent clear water sites, black squares represent forested sites, light blue triangles represent the vent, and dark blue inverted triangles represent the downstream bridge. DOC = dissolved organic carbon; PARAFAC = parallel factor analysis.

vent is apparent (e.g., DOC concentration in Figure 2a). Therefore, although the conduits encompassing sample sites V–VII appear to control the DOM exported from the Wakulla Springs vent, the relative contribution from clear water conduits and springs does play a role in determining the overall amount and quality of DOM exported. Thus, changing clear water inputs (e.g., reduced groundwater inputs) will have ramifications for DOC concentrations and CDOM content, as well as DOM composition at the vent and downstream.

In a wide array of past studies the relationship between CDOM and DOC has been examined in a range of ecosystems to investigate inputs of allochthonous and autochthonous DOM, as typically in systems dominated by allochthonous inputs strong correlations are observed between CDOM and DOC (Mann et al., 2012; Massicotte et al., 2017; Spencer et al., 2012). With respect to CDOM absorbance (a_{254}, a_{350}, and a_{440}) versus DOC concentrations the clear water sites (I–IV) exhibit statistically weak correlations (a_{254}: $r^2 = 0.078$, $p = 0.0048$; a_{350}: $r^2 = 0.010$, $p = 0.3166$; a_{440}: $r^2 = 0.002$, $p = 0.7186$; Table 3 and Figure 5a). There was no significant relationship between CDOM and DOC in clear water sites, as noted previously in other systems dominated by autochthonous and anthropogenic DOM sources (e.g., the Colorado and Rio Grande Rivers; Spencer et al., 2012). Conversely, CDOM absorbance (a_{254}, a_{350}, and a_{440}) versus DOC at forested sites (V–VII) exhibits statistically strong correlations (a_{254}: $r^2 = 0.913$, $p = <0.0001$; a_{350}: $r^2 = 0.905$, $p = <0.0001$; a_{440}: $r^2 = 0.848$; $p = <0.0001$; Table 3 and Figure 5b). The strong correlations seen at forested sites (V–VII) are indicative of predominantly allochthonous DOM, as seen in major U.S. and global rivers, and wetland ecosystems around the world (Mann et al., 2012; Massicotte et al., 2017; Spencer et al., 2012). The vent (site VIII) and downstream bridge (site IX) also showed similar trends as forested sites (V–VII) and exhibited statistically strong correlations between CDOM absorbance and DOC concentrations (e.g., for a_{350} $r^2 = 0.636$, $p = <0.0001$, and $r^2 = 0.951$, $p = <0.0001$, respectively; Table 3 and Figures 5c and 5d). As noted previously with respect to observed patterns in DOC and CDOM parameters (Table 2), here the similar correlations between CDOM and DOC observed at the vent and sites V–VII highlight these conduits as drivers of DOM quantity and quality at the Wakulla Springs vent.

In a similar vein to examination of CDOM and DOC relationships, FDOM was utilized to understand the sources of DOM in the vent and spring system by comparing PARAFAC components to DOC concentrations at all sites (Table 4 and Figure 6). With respect to C1 (humic-like), C2 (humic-like), and C3 (microbial humic-like) versus DOC concentrations, the forested sites (sites V–VII), the vent (site VIII), and the

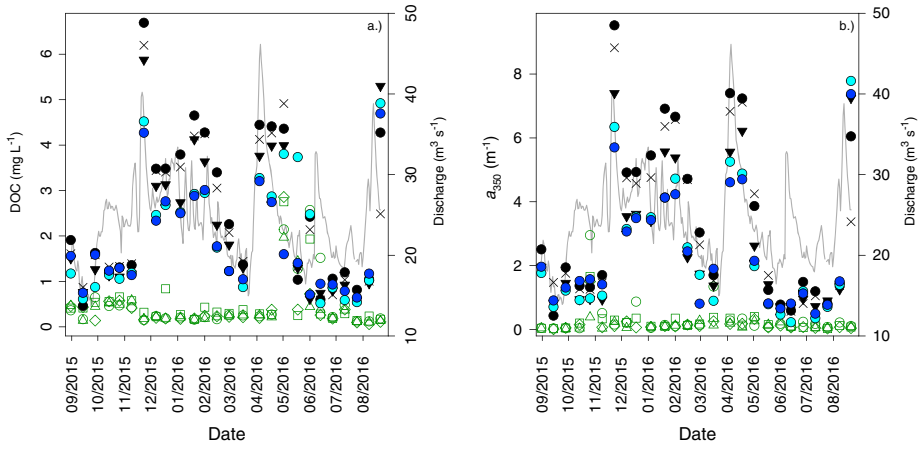

Figure 7. (a) Water discharge (Q) hydrograph for the Wakulla Springs river at the downstream bridge sample site versus DOC concentrations at each site throughout the year. (b) Water discharge (Q) for the Wakulla Springs river at the downstream bridge sample site versus a_{350} at each site throughout the year. Green symbols represent clear water sites, black symbols represent forested sites, light blue circles represent the Wakulla Springs vent, and dark blue circles represent the downstream bridge. DOC = dissolved organic carbon.

downstream bridge (site IX) showed strong correlations (e.g., C3: r^2 = 0.861, p = < 0.0001; r^2 = 0.650, p = <0.0001; and r^2 = 0.890, p = <0.0001, respectively; Table 4). This indicates that C1–C3 are associated with allochthonous DOM and with C2, which exhibits the most red-shifted emission maxima fluorophore, which has been linked to vascular plant sources (Coble et al., 1998; Fellman et al., 2010, supporting information Figure S1), showing the strongest correlation to DOC in the forested, vent, and bridge sites (Table 4). With respect to C4 (protein-like), C5 (microbial humic-like), and C6 (protein-like) versus DOC, there were no strong correlations among sample sites (Table 4, Figure 6). Of all the relationships between fluorescence components and DOC concentration for the clear water sites C6 showed the strongest relationship (r^2 = 0.308, p = < 0.0001; Table 4). Although not a robust relationship, it is unsurprising that protein-like fluorescence relates somewhat to DOC concentration in these clear groundwater-dominated sites as past studies have shown relationships between protein-like fluorescence and microbial sources of DOC (Baker, 2001; Baker et al., 2003, supporting information Table S1).

Table 5
Principal Components Analysis of the Nine Sample Sites, Component Matrix, and Variance Data

	Component	
Data	1	2
DOC (mg/L)	0.280	−0.059
a_{350} (m^{-1})	0.330	−0.210
$SUVA_{254}$ ($L \cdot mg\ C^{-1} \cdot m^{-1}$)	0.236	−0.159
a_{250}:a_{365}	−0.214	0.382
$S_{275-295}$ ($\times 10^{-3}\ nm^{-1}$)	−0.165	0.372
$S_{350-400}$ ($\times 10^{-3}\ nm^{-1}$)	−0.103	0.401
S_R	0.081	−0.355
FI	−0.319	0.036
HIX	0.310	0.246
BIX	−0.250	−0.191
%C1	0.224	0.316
%C2	0.331	0.197
%C3	0.281	0.150
%C4	−0.226	−0.266
%C5	−0.255	0.132
%C6	−0.228	−0.087
% of variance	43	19

Note. DOC = dissolved organic carbon; FI = fluorescence index; BIX = autotrophic productivity index; HIX = humification index; $SUVA_{254}$ = specific ultraviolet absorbance.

4.2. Influence of Seasonality on DOM Dynamics at Wakulla Springs

Water discharge (Q) data from the downstream bridge site (IX) showed seasonal variability driven predominantly by changes in flow from the vent (site VIII, Figure 7). Clear water sites (I–IV) showed little variation in DOC concentration throughout the year in respect to Q (Figure 7a), highlighting the stability of these groundwater inputs throughout the year (Xu et al., 2016). Forested sites (V–VII), the vent (VIII), and the downstream bridge (IX) all showed variability in DOC concentration with respect to Q. For example, these sites showed peaks in DOC concentration concurrent with major precipitation events in November 2015, and April and August 2016, as well as lower concentrations of DOC at periods of low flow (e.g., August–November 2015 and March 2015; Figure 7a). On comparisons of the downstream bridge DOC concentrations versus Q from that site (r^2 = 0.43, p = <0.001), it highlights that there is a response in relation to Q (i.e., precipitation) driven by inputs from the forested sites (V–VII) that is apparent at the vent (VIII) and downstream bridge (IX).

CDOM absorbance followed a similar trend to DOC concentration with respect to Q (Figure 7b). Clear water sites (I–IV) showed little variation in a_{350} throughout the year, while sites V–IX exhibited increased a_{350} values associated with precipitation events (Figure 7b) and a_{350} versus Q

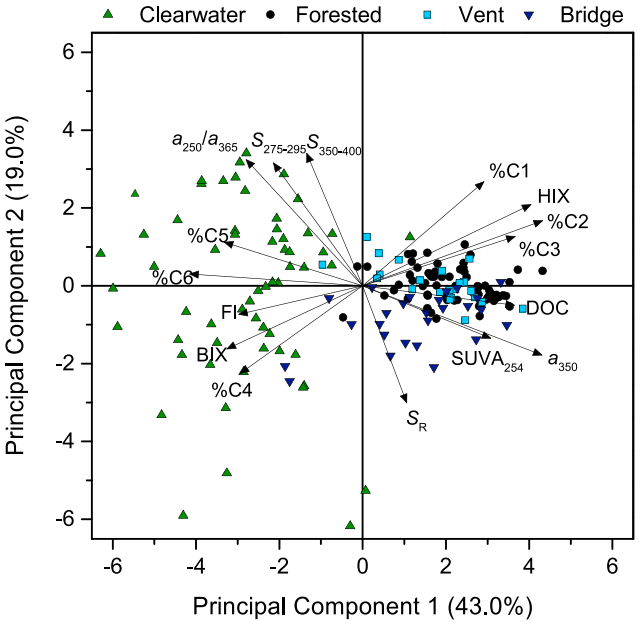

Figure 8. Principle component analysis of DOC concentrations and DOM compositional parameters for the Wakulla Springs conduit and vent ecosystem. DOC = dissolved organic carbon; DOM = dissolved organic matter.

(r^2 = 0.39, p = <0.001) shows a relationship with Q at the downstream bridge site (IX). The observed elevated DOC and a_{350} values concurrent with increased Q are indicative of different DOM source pools, hydrologic flow paths, and residence times at different times of year (Inamdar et al., 2006; McGlynn & McDonnell, 2003). This is particularly apparent at the high Q events post dry periods (November 2015, and April and August 2016), which exhibit the highest DOC and a_{350} values due to increased surface runoff and extensive leaching of organic-rich litters and surface soil layers at this time (Spencer et al., 2010; Striegl et al., 2005). The relatively stable DOC concentrations and DOM optical parameters observed at the clear water sites versus the forested sites and the similar response observed in the vent and bridge sites to the forested sites across the hydrograph further underpin the conduits encompassing sites V–VII as drivers of DOM at the Wakulla Springs vent (Table 2).

4.3. From Source to Vent: Drivers of DOM at Wakulla Springs

To further investigate the drivers of DOC concentration and DOM optical parameters in the Wakulla Springs conduit and vent ecosystem, a PCA was undertaken with log-transformed variables (Table 5 and Figure 8). Principle component one (PC1) explains 43% of the variance in the data and correlates positively with high values for a_{350}, DOC, $SUVA_{254}$, HIX, %C1, %C2, and %C3 and negatively with a_{250}:a_{365}, FI, BIX, %C4, %C5, and %C6 (Table 5). Therefore, it is apparent that PC1 relates to the separation of allochthonous-derived DOM versus autochthonous-derived DOM end-members. Principle component 2 (PC2) explains 19% of the variance in the data and correlates positively with $S_{275-350}$, $S_{350-400}$, a_{250}:a_{365}, and %C1 and negatively with S_R, a_{350}, BIX, and %C4 (Table 5). It appears that PC2 correlates to the seasonal variability in DOM composition found in the clear water sites (I–IV) that showed a particularly wide range of spectral slope parameter and a_{250}:a_{365} values, as well as relative contributions from fluorescence components C1 and C4 (Table 1 and Figures 3b and 4). This indicates there are sources of DOM to sites I–IV that impact the optical characteristics of the DOM pool typically found in these sites, which do not affect the forested sites, due to the greater variability observed on PC2 for the clear water sites (Figure 8). As sites I–IV encompass areas that drain from the city of Tallahassee and associated sources of anthropogenic contamination (Xu et al., 2016), one possibility is this variability in PC2 is driven by varying contributions from anthropogenic DOM sources. Past studies have shown the impact of even small amounts of sewage- and wastewater-derived DOM including optical brighteners such as those found in detergents, as well as landfill-derived leachates, and urban storm runoff on driving a wide variability in these optical parameters (Baker, 2001; Baker & Curry, 2004; Henderson et al., 2009; Zhao et al., 2015).

From the PCA there is a clear relationship between sites that are driven by terrestrially derived DOM versus predominantly groundwater sites exhibited by PC1 (Figure 8). The samples with the highest positive relationship on PC1 are those taken from forested sites (V–VII), vent (site VIII), and downstream bridge (IX) at elevated Q (Figure 7). The PCA clearly supports Table 2 demonstrating that the DOM discharging from the vent (site VIII) is largely derived from the conduits draining from the forested sites (V–VII) and explains the source of DOM and ultimately where the color (browning of the water) originates (Figure 8). Within PC1 there is a little overlap between the clear water and forested samples, and although the vent and bridge overlap for the majority of the year with the forested sites, they can be seen to overlap at times on PC1 with the clear water samples (Figure 8), representing periods of groundwater dominance from the vent concurrent with times of low Q. Overall, the results of the PCA indicate that optical (CDOM and FDOM) parameters are useful for delineating the dominant conduits with respect to export of DOM at the vent of Wakulla Springs and ultimately linking those conduits back to DOM sources. Similar approaches could be applied in other karst systems to assess changing CDOM inputs and their respective sources. Furthermore, future studies at this site or similar sites could combine characterization of DOM with commonly applied methods in identification and quantification of water sources centered on conservative tracers such as end-member mixing analysis or reaction network modeling (Arora et al., 2016; Barthold et al., 2011; Zhu, 2009).

As CDOM-rich water has become increasingly problematic at the Wakulla Springs vent in recent decades (Florida Geological Survey Special Publication 58, 2005), it seems apparent that either inputs from the conduits draining from the southwest including the Apalachicola National Forest within their catchment have increased or the relative dilution of this CDOM-rich water with optically clear groundwater in the conduit system has decreased. In recent years, studies have shown that a group of submarine springs (the Spring Creek Springs Complex) located to the south of Wakulla Springs has at times become a major site of seawater intrusion leading to a reverse in flow direction (Davis & Verdi, 2014; Xu et al., 2016). This in turn leads to the blackwater Lost Creek system, which typically transits southward when the Spring Creek Springs complex is flowing, to transit northward to Wakulla Springs bringing high CDOM water along with it (Dyer, 2015; Xu et al., 2016). As sea level in the region continues to rise, additional pressure head is placed on the Spring Creek Springs complex shifting flows including blackwater systems to Wakulla Springs (Davis & Verdi, 2014). Concurrent with this seawater intrusion, ongoing groundwater extraction throughout the springshed, particularly in the northern part of the aquifer, has increased fourfold in the last 50 years (Florida Springs Institute, 2014; Pratt et al., 1996) and further leads to a decline in clear water inputs (sites I–IV). Thus, with shifting sources to include more blackwaters linked to sea level rise, and ongoing reduction of clear waters due to extraction of groundwater for dilution of the CDOM-rich inputs, it appears that the increase in water color at the Wakulla Springs vent will persist and is directly related to anthropogenic impacts.

Acknowledgments
The authors would like to thank the Edward Ball Wakulla Springs State Park, Scott B. Dyer at the Florida Geological Survey, and the Northwest Florida Water Management District for their assistance. Thanks also go to Sarah Ellen Johnston, Travis Drake, Phoebe Zito, and Joan Pere Casas for fieldwork support. This work was partially supported by NSF (DMR-1157490), State of Florida, and the FSU Future Fuels Institute. F. G. was partly supported by a postdoctoral fellowship from the Fond de Recherche du Québec - Nature et Technologies. This study was supported by the Fish and Wildlife Foundation of Florida Protect Florida Springs grant PFS 1617-03. The data presented are listed in the tables and supporting information.

References

Aiken, G. R., Ksu-Kim, H., & Ryan, J. N. (2011). Influence of dissolved organic matter on the environmental fate of metals, nanoparticles and colloids. *Environmental Science & Technology*, *45*(8), 3196–3201. https://doi.org/10.1021/es103992s

Arellano, A. R., & Coble, P. G. (2015). Assessing carbon and nutrient inputs in a spring-fed estuary using fluorescence spectroscopy and discriminatory classification. *Limnology and Oceanography*, *60*(3), 789–804. https://doi.org/10.1002/lno.10078

Arora, B., Spycher, N. F., Steefel, C. I., Molins, S., Bill, M., Conrad, M. E., et al. (2016). Influence of hydrological, biogeochemical and temperature transients on subsurface carbon fluxes in a flood plain environment. *Biogeochemistry*, *127*(2-3), 367–396. https://doi.org/10.1007/s10533-016-0186-8

Baker, A. (2001). Fluorescence excitation-emission matrix characterization of some sewage-impacted rivers. *Environmental Science & Technology*, *35*(5), 948–953. https://doi.org/10.1021/es000177t

Baker, A., & Curry, M. (2004). Fluorescence of leachates from three contrasting landfills. *Water Research*, *38*, 2605–2613. https://doi.org/10.1016/j.waters.2004.02.027

Baker, A., & Genty, D. (1999). Fluorescence wavelength and intensity variations of cave waters. *Journal of Hydrology*, *217*(1–2), 19–34. https://doi.org/10.1016/S0022-1694(99)00010-4

Baker, A., Inverarity, R., Charlton, M., & Richmond, S. (2003). Detecting river pollution using fluorescence spectrophotometry: Case studies from Ouseburn, NE England. *Environmental Pollution*, *124*(1), 57–70. https://doi.org/10.1016/S0269-7491(02)00408-6

Baker, A., & Lamont-Black, J. (2001). Fluorescence of dissolved organic matter as a natural tracer of ground water. *Ground Water*, *39*(5), 745–750. https://doi.org/10.1111/j.1745-6584.2001.tb02365.x

Baker, A., & Spencer, R. G. M. (2004). Characterization of dissolved organic matter from source to sea using fluorescence and absorbance spectroscopy. *Science of the Total Environment*, *333*(1–3), 217–232. https://doi.org/10.1016/j.scitotenvi.2004.04.013

Barnes, K. K., Kolpin, D. W., Furlong, E. T., Zaugg, S. D., Meyer, M. T., & Barber, L. B. (2008). A national reconnaissance of pharmaceuticals and other organic wastewater contaminants in the United States—I. Groundwater. *Science of the Total Environment*, *402*(2–3), 192–200. https://doi.org/10.1016/j.scitotenv.2008.04.028

Barthold, F. K., Tyralla, C., Schneider, K., Vache, K. B., Frede, H. G., & Breuer, L. (2011). How many tracers do we need for endmember mixing analysis (EMMA)? A sensitivity analysis. *Water Resources Research*, *47*, W08519. https://doi.org/10.1029/2011WR010604

Berndt, M. P. (1990). Sources and distribution of nitrate in ground water at a farmed field irrigated with sewage treatment-plant effluent. Tallahassee, FL: U.S. Geological Survey Water-Resources Investigations Report, 90-4006.

Berndt, M. P., Oaksford, E. T., & Mahon, G. L. (1998). Groundwater, in Fernald, E.A. and Purdum, E.D., Water resources Atlas of Florida: Florida State University, Institute of Science and Public Affairs, 38-63.

Bianchi, T. S., Cook, R. L., Perdue, E. M., Kolic, P. E., Green, N., Zhang, Y., et al. (2011). Impacts of diverted freshwater on dissolved organic matter and microbial communities in Barataria Bay, Louisiana, U.S.A. *Marine Environmental Research*, *72*(5), 248–257. https://doi.org/10.1016/j.marenvres.2011.09.007

Birdwell, J. E., & Engel, A. S. (2009). Variability in terrestrial and microbial contributions to dissolved organic matter fluorescence in the Edwards Aquifer, Central Texas. *Journal of Cave and Karst Studies*, *71*(2), 144–156.

Birdwell, J. E., & Engel, A. S. (2010). Characterization of dissolved organic matter in cave and spring waters using UV-VIS absorbance and fluorescence spectroscopy. *Organic Chemistry*, *41*(3), 270–280. https://doi.org/10.1016/j.orggeochem.2009.11.002

Blough, N. V., & Del Vecchio, R. (2002). Chromophoric DOM in the coastal environment. In D. A. Hansell & C. A. Carlson (Eds.), *Biogeochemistry of marine dissolved organic matter* (pp. 509–546). San Diego, CA: Academic. https://doi.org/10.1016/B978-012323841-2/50012-9

Blough, N. V., & Green, S. A. (1995). Spectroscopic characterization and remote sensing of NLOM. In R. G. Zepp & C. Sonntag (Eds.), *The role of non-living organic matter in the Earth's carbon cycle* (pp. 23–45). NYC: John Wiley and Sons.

Blough, N. V., Zafiriou, O. C., & Bonilla, J. (1993). Optical absorption spectra of water from the Orinoco River outflow: Terrestrial input of colored organic matter to the Caribbean. *Journal of Geophysical Research*, *98*, 2271–2278. https://doi.org/10.1029/92JC02763

Bush, P. W., & Johnston, R. H. (1988). Ground-water hydraulics, regional flow, and ground-water development of the Floridan aquifer system in Florida and in parts of Georgia, South Carolina, USGS.

Chen, M., Price, R. M., Yamashita, Y., & Jaffé, R. (2010). Comparative study of dissolved organic matter from groundwater and surface water in the Florida coastal Everglades using multi-dimensional spectrofluorometry combined with multivariate statics. *Applied Geochemistry*, *25*(6), 872–880. doi.org/10.1016/j.apgeochem.2010.03.005

Coble, P. G., Del Castillo, C. E., & Avril, B. (1998). Distribution and optical properties of CDOM in the Arabian Sea during the 1995 SW monsoon. *Deep Sea Research Part II: Topical Studies in Oceanography*, *45*(10–11), 2195–2223. https://doi.org/10.1016/SO967-0645(98)00068-X

Coble, P. G., Green, S. A., Blough, N. V., & Gagosian, R. B. (1990). Characterization of dissolved organic matter in the Black Sea by fluorescence spectroscopy. *Nature*, *348*(6300), 432–435. https://doi.org/10.1038/348432a0

Cory, R. M., & McKight, D. M. (2005). Fluorescence spectroscopy reveals ubiquitous presence of oxidized and reduced quinones in DOM. *Environmental Science & Technology*, *39*(21), 8142–8149. https://doi.org/10.1021/es0506962

Cory, R. M., Miller, M. P., McKnight, D. M., Guerard, J. J., & Miller, P. L. (2010). Effect of instrument-specific response on the analysis of fluvic acid fluorescence spectra. *Limnology and Oceanography: Methods*, *8*(2), 67–78. https://doi.org/10.4319/lom.2010.8.67

Davis, J. H., & Verdi, R. (2014). Groundwater flow cycling between a submarine spring and an inland fresh water spring, *52* (5), 705–716. https://doi.org/10.1111/gwat.12125

Dyer, S. B. (2015). Dye tracing confirms conduit connect from Lost Creek Swallet to Spring Creek Springs and the Leon Sinks-Wakulla cave system, Florida State University, Thesis.

Fellman, J. B., Hood, E., D'Amore, D., Edwards, R. T., & White, D. (2009). Seasonal changes in the chemical quality and biodegradability of dissolved organic matter exported from soils to streams in coastal temperate rainforest watersheds. *Biogeochemistry*, *95*(2–3), 277–293. https://doi.org/10.1007/s10533-009-9336-6

Fellman, J. B., Hood, E., & Spencer, R. G. M. (2010). Fluorescence spectroscopy opens new windows into dissolved organic matter dynamics in freshwater ecosystems: A review. *Limnology and Oceanography*, *55*(6), 2452–2462. https://doi.org/10.4319/lo.2010.55.6.2452

Florida Geological Survey Special Publication 58 (2005). Degradation of water quality at Wakulla Springs, Florida: Assessment and recommendation.

Florida Springs Institute, Odum, T. H. (2014). Wakulla Spring a plan for the future. Retrieved from http://floridaspringsinstitute.org/Resources/Documents/2014.11%20Wakulla%20Restoration%20Executive%20Summary.pdf

Focazio, M. J., Kolpin, D. W., Barnes, K. K., Furlong, E. T., Meyer, M. T., & Zaugg, S. D. (2008). A national reconnaissance for pharmaceuticals and other organic wastewater contaminants in the United States—II. Untreated drinking water sources. *Science of the Total Environment*, *402*(2–3), 201–216. https://doi.org/10.1016/j.scitotevn.2008.02.021

Guéguen, C., Cuss, C. W., Cassels, C. J., & Carmack, E. C. (2014). Absorption and fluorescence of dissolved organic matter in the waters of the Canadian Arctic archipelago, Baffin Bay, and the Labrador Sea. *Journal of Geophysical Research: Oceans*, *119*, 2034–2047. https://doi.org/10.1002/2013JC009173

Hartmann, A., Goldscheider, N., Wagener, T., Lange, J., & Weiler, M. (2014). Karst water resources in a changing world: Review of hydrological modeling approaches. *Reviews of Geophysics*, *52*, 218–242. https://doi.org/10.1002/2013RG000443

Helms, J. R., Aron, S., Jason, D. R., Minor, E. C., Kieber, D. J., & Mopper, K. (2008). Absorption spectral slopes and slope ratios as indicators of molecular weight, source, and photobleaching of chromophoric dissolved organic matter. *Limnology and Oceanography*, *53*(3), 955–969. https://doi.org/10.4319/lo.2008.53.3.0955

Henderson, R. K., Baker, A., Murphy, K. R., Hambly, A., Stuetz, R. M., & Khan, S. J. (2009). Fluorescence as a potential monitoring tool for recycled water systems: A review. *Water Research*, *43*. https://doi.org/10.1016/j.watres.2008.11.027

Hudson, N., Baker, A., & Reynolds, D. (2007). Fluorescence analysis of dissolved organic matter in natural, waste and polluted waters—A review. *River Research and Applications*, *23*(6), 631–649. https://doi.org/10.1002/rra.1005

Huguet, A., Vacher, L., Relexans, S., Saubusse, S., Froidefond, J. M., & Parlanti, E. (2009). Properties of fluorescent dissolved organic matter in the Gironde estuary. *Organic Geochemistry*, *40*(6), 706–719. https://doi.org/10.1016/j.orggeochem.2009.03.002

Inamdar, S. P., O'Leary, N., Mitchell, M. J., & Riley, J. T. (2006). The impact of storm events on solute exports from a glaciated forested watershed in western New York, USA. *Hydrological Processes*, *20*(16), 3423–3439. https://doi.org/10.1002/hyp.6141

Jaffé, R., McKnight, D., Maie, N., Cory, R., McDowell, W. H., & Campbell, J. L. (2008). Spatial and temporal variations in DOM composition in ecosystems: The importance of long-term monitoring of optical properties. *Journal of Geophysical Research*, *113*, G04032. https://doi.org/10.1029/2008JG000683

Johnson, M. S., Couto, E. G., Abdo, M., & Lehmann, J. (2011). Fluorescence index as an indicator of dissolved organic carbon quality in hydrologic flowpaths of forested tropical watersheds. *Biogeochemistry*, *105*(1–3), 149–157. https://doi.org/10.1007/s10533-011-9595-x

Katz, B. G., & Griffin, D. W. (2008). Using chemical and microbiological indicators to track the possible movement of contaminants from the land application of treated municipal wastewater and other sources on groundwater quality in a karstic springs basin. *Environmental Geology*, *55*(4), 801–821. https://doi.org/10.1007/s00254-007-1033-y

Kothawala, D. N., Murphy, K. R., Stedmon, C. A., Weyhenmeyer, G. A., & Tranvik, L. J. (2013). Inner filter correction of dissolved organic matter fluorescence. *Limnology and Oceanography: Methods*, *11*(12), 616–630. https://doi.org/10.4319/lom.2013.11.616

Kothawala, D. N., Stedmon, C. A., Müller, R. A., Weyhenmeyer, G. A., Köhler, S. J., & Tranvik, L. J. (2014). Controls of dissolved organic matter quality: Evidence form a large-scale boreal lake survey. *Global Change Biology*, *20*(4), 1101–1114. https://doi.org/10.1111/gcb.12488

Kothawala, D. N., von Wachenfeldt, E., Koehler, B., & Tranvik, L. J. (2012). Selective loss and preservation of lake water dissolved organic matter fluorescence during long-term dark incubations. *Science of the Total Environment*, *433*, 238–246. https://doi.org/10.1016/j.scitotenv.2012.06.029

Mann, P. J., Davydova, A., Zimov, N., Spencer, R. G. M., Davydov, S., Bulygina, E., et al. (2012). Controls on the composition and lability of dissolved organic matter in Siberia's Kolyma River basin. *Journal of Geophysical Research*, *117*, G01028. https://doi.org/10.1029/2011JG001798

Massicotte, P., Asmala, E., Stedmon, C., & Markager, S. (2017). Global distribution of dissolved organic matter along the aquatic continuum: Across rivers, lakes, and oceans. *Science of the Total Environment*, *609*, 180–191. https://doi.org/10.1016/j.scitotenv.2017.07.076

McGlynn, B. L., & McDonnell, J. J. (2003). Role of discrete landscape units in controlling catchment dissolved organic carbon dynamics. *Water Resources Research*, *39*(4), 1090. https://doi.org/10.1029/2002WR001525

McKnight, D. M., Boyer, E. W., Westerhoff, P. K., Doran, P. T., Kulbe, T., & Anderson, D. T. (2001). Spectrofluorometric characterization of dissolved organic matter for indication of precursor organic material and aromaticity. *Limnology and Oceanography*, *46*(1), 38–48. https://doi.org/10.4319/lo.2001.46.1.0038

Murphy, K. R. (2011). A note on determining the extent of the water Raman peak in fluorescence spectroscopy. *Applied Spectroscopy*, *65*(2), 233–236. https://doi.org/10.1366/10-06136

Murphy, K. R., Stedmon, C. A., Graeber, D., & Bro, R. (2013). Fluorescence spectroscopy and multi-way techniques. PARAFAC. *Analytical Methods*, *5*(23), 6557–6566. https://doi.org/10.1039/C3AY41160E

Musgrove, M., Opsahl, S. P., Mahler, B. J., Herrington, C., Sample, T. L., & Banta, J. R. (2016). Source, variability, and transformation of nitrate in a regional karst aquifer: Edwards aquifer, central Texas. *Science of the Total Environment*, *568*, 457–469. https://doi.org/10.1016/j.scitotenv.2016.05.201

Ohno, T. (2002). Fluorescence inner-filter correction for determining the humification index of dissolved organic matter. *Environmental Science & Technology*, *36*(4), 742–746. https://doi.org/10.1021/es0155276

Osburn, C. L., Wigdahl, C. R., Fritz, S. C., & Saros, J. E. (2011). Dissolved organic matter composition and photoreactivity in prairie lakes of the U. S. Great Plains. *Limnology and Oceanography*, *56*(6), 2371–2390. https://doi.org/10.4319/lo.2011.56.6.2371

Para, J., Coble, P. G., Chariére, B., Tedetti, M., Fontana, C., & Sempére, R. (2010). Fluorescence and absorption properties of chromophoric dissolved organic matter (CDOM) in coastal surface waters of the northwestern Mediterranean Sea, influence of the Rhône River. *Biogeosciences*, *7*(12), 4083–4103. https://doi.org/10.5194/bg-7-4083-2010

Peuravuori, J., & Pihlaja, K. (1997). Molecular size distribution and spectroscopic properties of aquatic humic substances. *Analytica Chimica Acta*, *337*(2), 133–149. https://doi.org/10.1016/S0003-2670(96)00412-6

Pratt, T. R., Richards, C. J., Milla, K. A., Wagner, J. R., Johnson, J. L., & Curry, R. J. (1996). Hydrogeology of the northwest Florida water management district. *Water Resources Special Report*, *96-4*, 98.

Regan, S., Hynds, P., & Flynn, R. (2017). An overview of dissolved organic carbon in groundwater and implications for drinking water safety. *Hydrogeology Journal*, *25*(4), 959–967. https://doi.org/10.1007/s10040-017-1583-3

Shank, G. C., & Evans, A. (2011). Distribution and photoreactivity of chromophoric dissolved organic matter in northern Gulf of Mexico shelf waters. *Continental Shelf Research*, *31*(10), 1128–1139. https://doi.org/10.1016/j.csr.2011.04.009

Shen, Y., Chapelle, F. H., Strom, E. W., & Benner, R. (2015). Origins and bioavailability of dissolved organic matter in groundwater. *Biogeochemistry*, *122*(1), 61–78. https://doi.org/10.1007/s10633-014-0029-4

Sophocleous, M. (2002). Interactions between groundwater and surface water: The state of the science. *Journal of Hydrology*, *10*, 52–67.

Spencer, R. G. M., Aiken, G. R., Butler, K. D., Dornblaser, M. M., Striegl, R. G., & Hernes, P. J. (2009). Utilizing chromophoric dissolved organic matter measurements to derive export and reactivity of dissolved organic carbon to the Arctic Ocean: A case study of the Yukon River, Alaska. *Geophysical Research Letters*, *36*, L06401. https://doi.org/10.1029/2008GL036831

Spencer, R. G. M., Aiken, G. R., Wickland, K. P., Striegl, R. G., & Hernes, P. J. (2008). Seasonal and spatial variability in dissolved organic matter quantity and composition from the Yukon River basin, Alaska. *Global Biogeochemical Cycles*, *22*, GB4002. https://doi.org/10.1029/2008GB003231

Spencer, R. G. M., Butler, K. D., & Aiken, G. R. (2012). Dissolved organic carbon and chromophoric dissolved organic matter properties of rivers in the USA. *Journal of Geophysical Research*, *117*, G03001. https://doi.org/10.1029/2011JG001928

Spencer, R. G. M., Hernes, P. J., Ruf, R., Baker, A., Dyda, R. Y., Stubbins, A., & Six, J. (2010). Temporal controls on dissolved organic matter and lignin biogeochemistry in a pristine tropical river, Democratic Republic of Congo. *Journal of Geophysical Research*, *115*, G03013. https://doi.org/10.1029/2009JG001180

Spencer, R. G. M., Stubbins, A., Hernes, P. J., Baker, A., Mopper, K., Aufdenkampe, et al. (2009). Photochemical degradation of dissolved organic matter and dissolved lignin phenols from the Congo River. *Journal of Geophysical Research*, *114*, G03010. https://doi.org/10.1029/2009JG000968

Stedmon, C. A., Amon, R. M. W., Rinehart, A. J., & Walker, S. A. (2011). The supply and characteristics of colored dissolved organic matter (CDOM) in the Arctic Ocean: Pan Arctic trends and differences. *Marine Chemistry*, *124*(1–4), 108–118. https://doi.org/10.1016/j.marchem.2010.12.007

Stedmon, C. A., Markager, S., & Bro, R. (2003). Tracing dissolved organic matter in aquatic environments using a new approach to fluorescence spectroscopy. *Marine Chemistry*, *82*(3–4), 239–254. https://doi.org/10.1016/S0304-4203(03)00072-0

Striegl, R. G., Aiken, G. R., Dornblaser, M. M., Raymond, P. A., & Wickland, K. P. (2005). A decrease in discharge-normalized DOC export by the Yukon River during summer through autumn. *Geophysical Research Letters*, *32*, L21413. https://doi.org/10.1029/2005GL024413

United States Geological Survey (USGS) (2018). 02327022 Wakulla River near Crawfordville, FL. https://waterdata.usgs.gov/usa/nwis/dvstat/?site_no=02327022&por_02327022_26830=2396655,00060,26830

Wang, Y., Zhang, D., Shen, Z., Chen, J., & Feng, C. (2014). Characterization and spatial distribution variability of chromophoric dissolved organic matter (CDOM) in the Yangtze estuary. *Chemosphere*, *95*, 353–362. https://doi.org/10.1016/j.chemosphere.2013.09.044

Weishaar, J. L., Aiken, G. R., Bergamaschi, B. A., Fram, M. S., Fujil, R., & Mopper, K. (2003). Evaluation of specific ultraviolet absorbance as an indicator of the chemical composition and reactivity of dissolved organic carbon. *Environmental Science and Technology*, *37*(20), 4702–4708. https://doi.org/10.1021/es030360x

Xu, Z., Bassett, S. W., Hu, B. X., & Dyer, S. B. (2016). Long distance seawater intrusion through a karst conduit network in the Woodville karst plain, Florida. *Scientific Reports*, *6*(1), 1–9. https://doi.org/10.1038/srep32235

Xu, Z., Hu, B. X., Davis, H., & Cao, J. (2015). Simulating long term nitrate-N contamination processes in the Woodville karst plain using CFPv2 with UMT3D. *Journal of Hydrology*, *524*, 72–88. https://doi.org/10.1016/J.hydrol.2015.02.024

Zhao, C., Wang, C., Li, J., Wang, C., Wang, P., & Pei, Z. (2015). Dissolved organic matter in urban stormwater runoff at three typical regions in Beijing: Chemical composition, structural characterization and source identification. *RSC Advances*, *5*(90), 73,490–73,500. https://doi.org/10.1039/C5RA14993B

Zhu, C. (2009). Geochemical modeling of reaction paths and geochemical reaction networks. *Reviews in Mineralogy and Geochemistry*, *70*(1), 533–569. https://doi.org/10.2138/rmg.2009.70.12

Zsolnay, A., Baigar, E., Jimenez, M., Steinweg, B., & Saccomandi, F. (1999). Differentiating with fluorescence spectroscopy the sources of dissolved organic matter in soils subjected to drying. *Chemosphere*, *38*(1), 45–50. https://doi.org/10.1016/S0045-6535(98)00166-0